RSC Advances

PAPER

View Article Online
View Journal | View Issue

Cite this: *RSC Adv.*, 2017, **7**, 42233

Degradation of aquatic sulfadiazine by Fe^0/persulfate: kinetics, mechanisms, and degradation pathway†

Shidong Yang * and Di Che

Effects of treatment factors on the kinetics of sulfadiazine (SDZ) removal by Fe^0/persulfate (Fe^0/PS) were studied at an initial pH of 7.0. The kinetics of SDZ degradation by Fe^0/PS were divided into a lag phase and a rapid reaction. The presence of the lag phase was ascribed to the slow release of Fe(II) in the heterogeneous Fe^0/PS system. The rapid phase was simulated by pseudo first-order kinetics model. With increasing Fe^0 or PS ranging from 0.25 to 2 mM, the k_{obs} (min^{-1}) of SDZ degradation increased and remained stable at a high level of 5 mM Fe^0 or PS. But increasing SDZ inhibited the SDZ removal rate for the scavenging of reactive oxygen species (ROS). SDZ degradation by Fe^0/PS in neutral or weak alkaline solutions exhibited higher removal rates than in weak acid solutions. Common aquatic materials including sulfate, nitrate, chloride, perchlorate, and HA all showed negative effects on SDZ degradation by Fe^0/PS following a trend of $Cl^- < ClO_4^- < SO_4^{2-} < NO_3^- < HCO_3^- <$ HA. The dominating ROS in the Fe^0/PS system was identified as $^{\bullet}SO_4^-$ by chemical quenching experiments in the presence of methanol or *tert*-butyl alcohol. And the chemical detection of dimethyl pyridine *N*-oxide (DMPO)-$^{\bullet}SO_4^-$ and DMPO–$^{\bullet}OH$ by electron paramagnetic resonance (EPR) spectrum confirmed the presence of $^{\bullet}SO_4^-$. Besides, strongly negative effects of 1,10-phenanthroline, ethylenediaminetetraacetic acid (EDTA), and dissolving oxygen (DO) on SDZ degradation in the Fe^0/PS process proved that $^{\bullet}SO_4^-$ was not generated by an one-step reaction between Fe^0 and PS but *via* the indirect oxidation of Fe(II) by PS. Finally, degradation pathways of SDZ by Fe^0/PS were proposed based on theoretical reactive sites attacked by radicals and intermediate products.

Received 18th July 2017
Accepted 24th August 2017

DOI: 10.1039/c7ra07920f

rsc.li/rsc-advances

Introduction

Sulfonamide drugs have been synthesized and commercially used since 1930s.[1] This important category of antibiotics has been extensively used to treat and prevent various infectious diseases of humans and animals due to its broad antimicrobial spectrum.[2] According to the reports of Zhang *et al.*,[1] 7136 tons of 9 typical sulphonamides were consumed in China in 2013, about 94.3% of which were used as veterinary antibiotics for pigs, chicken, and other animals. The over-use of sulfonamides, especially in the industry of livestock feeding,[3] has increased the potential contamination of sulfonamides in water and soil environments. Most sulfonamides are excreted from the human body and animal organisms partially in unmetabolised form.[4] Many studies have revealed that the expired and unused sulfonamides exposed to humans have shown various adverse effects towards human health.[5] Although sulfonamides in ground and surface water are detected at low levels,[6] residual sulfonamides can be accumulated in various organisms of a food chain, increasing antibiotic resistance of pathogenic bacteria in aquatic environments.[7]

Traditional wastewater treatment plants (WWTPs) using biological technologies as the main processes may be ineffective to sulphonamides for the aquatic sulphonamides exhibit high resistance to biological degradation as antibiotics.[8] Many researchers[2,9,10] have reported that the removal rates of various sulfonamides by traditional WWTPs are limited, thus adopting effective treatment alternatives is essential to eliminate the contamination of sulfonamides.

Of various chemical techniques, such as advance oxidation process (AOPs),[11] ozonation,[12] and permanganate,[13] AOPs have been frequently employed to remove many antibiotics in water and wastewater treatment processes since hydroxyl radical ($^{\bullet}OH$) produced by AOPs possesses stronger redox potential ($E^0 = 1.9$–2.7 V),[14] higher performance, and superior mineralization rate than traditional chemical oxidants.[15] In recent years, new AOPs based on sulfate radical ($^{\bullet}SO_4^-$) have been developed to destroy organic pollutants include antibiotics[16] and dyes[17] in surface water,[18,19] hospital effluents,[20] and waste water.[21] Sulfate radical has been known as a strong oxidant for its higher redox

School of Civil Engineering and Architecture, Northeast Electric Power University, Jilin 132012, PR China. E-mail: ysd_nedu@163.com; Fax: +86-432-64806481; Tel: +86-432-64806481

† Electronic supplementary information (ESI) available. See DOI: 10.1039/c7ra07920f

potential (E^0 = 2.5–3.1 V)[14] than hydroxyl radical. Moreover, Neta *et al.*[22] has reported that sulfate radical is a more effective oxidant than hydroxyl radical to eliminate many organic compounds by hydrogen abstraction and addition in a wide pH range. Thus, the AOP based on sulfate radical was an effective strategy to degradative aquatic sulfonamides.

The activation of persulfate (PS) and peroxymonosulfate (PMS) have been considered as the most portable methods to generate sulfate radical in aquatic environment. PS occupying higher redox potential (E^0 = 2.01 V)[23] have been widely used to generate $^{\cdot}SO_4^-$ when it is activated by transition metals and heterogeneous catalysts. Among various transition metal ions, Fe(II) is advantageous since it is cheap, non-toxic, naturally abundant and environmental friendly.[19] Classical Fe(II) activating PS process has present potential efficiencies on rapidly reducing and even mineralizing organics for the generation of sulfate radical *via* eqn (1), but a higher removal rate of the target compound requires the continuous addition of dissolved Fe(II) in a homogeneous system.[19] Meanwhile, excessive Fe(II) can quickly consume PS or sulfate radical in solution, which can seriously inhibit removal efficiency of target organics (Eq. (2)). Recently, zero valent iron (ZVI, Fe^0), as a green reductive reagent,[24–28] *in lieu* of Fe(II) can also induce heterogeneous activated PS, and some studies of sulfamethoxazole degradation by Fe^0/PS have been reported by Ghauch's group.[29,30] The application of Fe^0 not only overcome the disadvantages of sulfate radical and PS consumption by excessive Fe(II) but also avoid the addition of other anions (Cl^- or SO_4^{2-}) to the solution (Eq. (1) and (3)). Meanwhile, the recycle of Fe(II) by the reaction between Fe(II) and Fe^0 at the Fe^0 surface has been provided (Eq. (4)). According to Oh *et al.*,[31] Fe^0 not only is the source of dissolved Fe(II), but also directly activates PS to produce sulfate radical which did not transform to Fe(II) (Eq. (5)). Besides, Guo *et al.*[12,32] firstly reported that common oxidants could enhance the reactivity of Fe^0 by cleaning the precipitation of ferric hydroxides at the Fe^0 surface. Lai *et al.*[33,34] also reported that the PS could accelerate the reductive rate of 4-nitrophenol by Fe^0. Thus Fe^0 exhibiting more reactivity in the presence of PS also can generate $^{\cdot}OH$ rather than $^{\cdot}SO_4^-$ with dissolved oxygen in aquatic chemistry. Thus, the dominating ROS in the Fe^0/PS process should be identified, and the reactive mechanisms between Fe^0 and PS need to be reinvestigated.

$$S_2O_8^{2-} + Fe^{2+} \rightarrow {}^{\cdot}SO_4^- + Fe^{3+} + SO_4^{2-} \quad (1)$$

$$^{\cdot}SO_4^- + Fe^{2+} \rightarrow Fe^{3+} + SO_4^{2-} \quad (2)$$

$$Fe^0 - 2e^- \rightarrow Fe^{2+} \quad (3)$$

$$Fe^0 + 2Fe^{3+} \rightarrow 3Fe^{2+} \quad (4)$$

$$2S_2O_8^{2-} + Fe^0 \rightarrow 2{}^{\cdot}SO_4^- + Fe^{2+} + 2SO_4^{2-} \quad (5)$$

Hence, sulfadiazine (SDZ) as a typical sulfonamide was selected as the target containment, and kinetics, mechanisms, and degradation pathway of SDZ degradation in the Fe^0/PS process were investigated. The aims of this study are to (1) assess the effects of initial Fe^0, PS, and SDZ concentration on SDZ degradation by the Fe^0/PS process, (2) determine the effects of several background materials in water on SDZ degradation by the Fe^0/PS process, (3) identify the dominating ROS in the Fe^0/PS process, and (4) clarify SDZ degradation pathways in the Fe^0/PS process.

Experimental

Materials

Sulfadiazine of 99% purity was supplied by TCI Co. LLC. (Tokyo, Japan). Fe^0 powder of 97% purity, dimethyl pyridine *N*-oxide (DMPO) of 97% purity, and humic acid (HA) were purchased from Sigma-Aldrich Co. LLC. (St. Louis, MO, USA). Potassium persulfate were supplied by Sinopharm Chemicals Reagent Co., Ltd. (Shanghai, China). Other chemicals of analytical grade were provided by Sinopharm Chemicals Reagent Co., Ltd. All chemicals were not further purified and solutions were prepared with deionized (DI) water.

Batch experiments

Kinetic experiments were carried out in an organic glass reactor open to the air at 20 ± 1.0 °C, and 0.5 L solution containing SDZ was completely mixed by digital display electric blender at 600 rotation rate (rpm). For experiments carried out under anoxic and oxygen conditions, solutions were purged for 30 min including 20 min of preparation time and 10 min of reaction time with pure nitrogen and oxygen at a flow rate of 1 L min^{-1} controlled by VAT-315 rotary flowmeter (Dwyer Instruments Inc., US), respectively. The initial pH of solution was adjusted by H_2SO_4 and NaOH, and then experiments were initiated after addition of Fe^0 and PS into the reactor. For the kinetic study, at fixed time intervals, 2 mL sample was rapidly transferred into the sample beaker that was immediately quenched with 20 μL of sodium hyposulfite, filtered with 0.22 μm membrane and collected into sample vials quickly.

Chemical analysis

A Mettler-Toledo high-performance FE20-FiveEasy pH meter with a saturated KCl solution as electrolyte produced (Switzerland) was employed to measure solution pH and daily calibration with standard buffers (pH 4.00, 6.86 and 9.18) was done to ensure its accuracy. Electron paramagnetic resonance (EPR) spectrometry (Bruker, Germany) with the magnetic field of 3400–3500 G was employed.

A Merlin Compact scanning electron microscopy (SEM) (Carl Zeiss, Germany) coupled with an X-Max energy dispersive X-ray spectrum (Oxford Instrument, UK) was employed to characterize iron particles and analysis the elemental composition which were depicted in Fig. S1 (see ESI†). The concentrations of Fe(II) and total ions (after reduction to Fe(II) with hydroxylamine hydrochloride) were determined at 510 nm after complexing with 1,10-phenanthroline by an UV-2600 UV-Vis spectrophotometer (Shimadzu, Japan).

SDZ was determined by a Waters ACQUITY ultra-performance liquid chromatography (UPLC) system including a binary solvent manager and a sample manager with a TUV

detector (Milford MA, United States). The water samples were extracted by an off line solid-phase extraction (SPE) with Oasis HLB (200 mg) cartridges which was used to enrich and to clean up the aqueous sample. Separation was accomplished with an Agilent SB-C18 column (2.1 × 50 mm, 1.8 μm; Agilent, United States) at 30 ± 1.0 °C with a mobile phase of two effluents (effluent A: 30% acetonitrile; effluent B: 70% H_2O with 0.1% formic acid) at a flow rate of 0.1 mL min^{-1}. Concentrations of SDZ were determined by comparing the peak area at 265 nm with that of standards. The intermediate products of SDZ degradation were separated by the Agilent 1290 Infinity but interfaced with a triple quadrupole mass detector (6400) (UHPLC-MS) (Santa Clara CA, United States). The separated sample analysis by mass spectra was conducted in positive and negative mode electrospray ionization ((+)ESI and (−)ESI) over a mass range of 50–500 *m*/*z*. Separation was accomplished with an Agilent Proshell-C18 column (2.1 × 100 mm, 1.8 μm; Agilent, United States). The fragment used was 90 V conducted in auto full scan mode (MS). The fragment and collision energy used in product ion mode were 90 V and 15 eV, respectively.

Results and discussion

Effects of treatment factors on kinetics of SDZ removal in the Fe^0/PS process

The effect of initial Fe^0 loading ranged from 0.25 to 5 mM on kinetics of SDZ degradation in the Fe^0/PS process is shown in Fig. 1(a). SDZ degradative curve by Fe^0/PS exhibited an auto-catalytic shape, which was divided into a lag phase and a rapid degradation phase in the Fe^0/PS process similar to the Fe^0/H_2O_2 process.[35] The lag phase was explained by heterogeneous reactions between Fe^0 and PS, and was shortened with increasing Fe^0 loading. Then rapid reactions between Fe(II) and PS was initialled by the releasing of Fe(II) after the lag phase. The degradative rate constant of SDZ by Fe^0/PS in the rapid phase is calculated by a pseudo-first-order kinetic model (Eq. (6)),[8] and fitting results are shown as solid lines in Fig. 1.

$$-\frac{d[SDZ]}{dt} = k_{obs}[SDZ] \quad (6)$$

where k_{obs} is the pseudo-first-order rate constant (min^{-1}) of SDZ removal by Fe^0/PS, and [SDZ] represents the concentration of SDZ.

The rate constant of SDZ removal linearly increases with Fe^0 loading ranged from 0.25 mM to 2 mM (see Fig. S2(a)†) for more Fe^0 could release more Fe(II). The final removal rate of SDZ at 10 min also increased with initial Fe^0 loading. When the concentration of Fe^0 reached 5 mM, the rate constant of SDZ removal did not increase but even slightly decreased from 0.63 to 0.58 min^{-1} that was ascribed to the consumption of ROS by excess Fe^0. Similarly, the final removal rate of SDZ at 10 min merely rose about 2% from with increasing Fe^0 loading from 2 to 5 mM. As shown in Fig. 1(b), the influence of initial PS concentration ranged from 0.25 to 5 mM in SDZ removal kinetics by Fe^0/PS was investigated. The lag phase was seriously shortened to 1 min with PS of high concentration above 1 mM. Increasing PS could rapidly eliminate the passivating film on

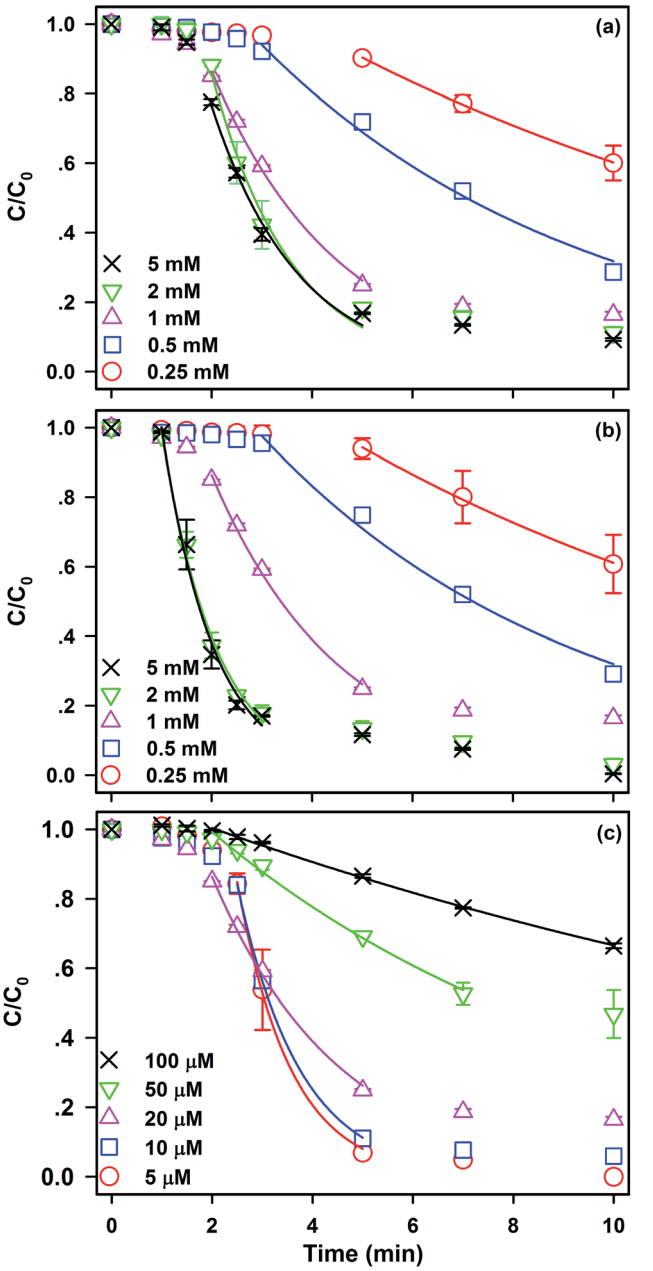

Fig. 1 Effect of initial Fe^0 loading (a), PS concentration (b), and SDZ concentration (c) on SDZ degradative kinetics by Fe^0/PS. Experimental conditions: initial pH = 7.0, rpm = 600, and T = 20 ± 1 °C.

the surface of Fe^0 and improved the reactivity of Fe^0. According to eqn (1), more PS could accelerate reactions between Fe(II) and PS by generating more ROS. Thus, the rate constant of SDZ removal linearly increase with increasing PS concentration from 0.25 mM to 2 mM (see Fig. S2(a)†). In addition, the degradative rate constant of SDZ in rapid phase and the removal rate of SDZ was not increased with increasing PS from 2 to 5 mM for the limitation of Fe^0 loading.

Influence of SDZ concentration on SDZ removal by Fe^0/PS also are studied in Fig. 1(c). At low SDZ concentration, the rate constant of SDZ removal was not changed. With increasing SDZ concentration above 10 μM, the rate constant and removal rate

of SDZ degradation were seriously inhibited for the amount of ROS was limited to concentrations of Fe^0 and PS. Thereby, removal of aquatic SDZ of high concentrations might require more Fe^0 and PS.

Meanwhile, a comparison of SDZ removal kinetics in the Fe^0/PS system and the Fe(II)/PS system has been conducted in Fig. S3† at the optimal experimental conditions. Fe(II) showed the high activity towards PS in the first 1 min, which was different from the lag phase in the Fe^0/PS system. But the final removal rate of SDZ by Fe(II)/PS was lower than Fe^0/PS for the consumption of ROS by excess dissolving Fe(II), which was in agreement with other reports.[29]

Effect of initial pH

Generally, pH value plays a key role in the application of traditional AOPs.[19] Hence, the effect of initial pH on SDZ degradation in the Fe^0/PS process should be clarified. As illustrated in Fig. 2, SDZ degradative kinetics by Fe^0/PS in a wide range of initial pH value from 5.0 to 9.0 are investigated. Meanwhile, the variation of pH values in the reaction has been monitored in Fig. S4†(a). The acid solution could shorten the lag phase and accelerate the rate constant of SDZ degradation since Fe^0 showed more activity in weak acid conditions. Nevertheless, the final removal rate of SDZ were only 70.4% at pH 5.0 and 69.4% at pH 6.0, which were much lower than that of 83.5% at neutral pH. Quick release of Fe(II) in acid solutions might enhance reactions between Fe(II) and PS but excess Fe(II) seriously compete for ROS or PS with SDZ. On the contrary, alkaline solutions at pH 8.0 and 9.0 can restrain the passivation of Fe^0 surface and extend the lag phase of SDZ. The degradative kinetics and the rate constant of SDZ removal in the rapid phase at pH 8.0–9.0 still reach 0.28 min^{-1} which is lower than 0.40 min^{-1} at pH 7.0 (see Fig. S4†(b)). Nevertheless, the presence of PS could accelerate the passivation of Fe^0 as reported by Lai,[33,34] and the Fe^0/PS system in alkaline solutions still developed reactive ability to degrade SDZ. Therefore, the removal rate at 10 min did not decrease with increasing pH. Removal rates of SDZ by Fe^0/PS in alkaline and neutral solutions were even higher than that at acid pH, which indicated that alkaline solutions did not decrease the total concentration of ROS employed to destroy SDZ. So slow release of Fe(II) rather than rapid dissolving Fe(II) from Fe^0 enhanced the degradative reactions between ROS and SDZ in the Fe^0/PS process. Neutral and weak alkaline pH are more suitable to SDZ degradation by Fe^0/PS, which increase the potential for engineering applications in organics removal in the Fe^0/PS process. Furthermore, sludge generation by the end of the reaction was well controlled in neutral and weak alkaline pH by comparing with the concentration of dissolved iron species in solution at each pH (see Fig. S4(b)†).

Effects of background materials in water on SDZ removal by Fe^0/PS

Batch experiments were carried out to investigate SDZ degradative kinetics by Fe^0/PS in the presence of aquatic background materials including Cl^-, SO_4^{2-}, NO_3^-, ClO_4^-, HCO_3^-, and HA. The raw time courses of SDZ removal by Fe^0/PS are shown and modelled by eqn (1) in Fig. S5.† The summary of rate constants are exhibited in Fig. 3. With increasing sulfate, the inhibition on SDZ degradation increased for the reactivity of ZVI for the precipitation of acicular α-FeOOH and precipitation of basic ferric sulfate on iron surface.[36] Meanwhile, the presence of SO_4^{2-} might also decrease the redox potential of $^{\cdot}SO_4^-/SO_4^{2-}$, and weaken the oxidative activity of PS.[37] Nitrate anion always exhibited serious inhibiting effects on SDZ removal by Fe^0/PS with increasing nitrate.[24] Nitrate was easily reduced by Fe^0 and the reactivity between Fe^0 and PS was decreased for the competition of nitrate.[38] Besides, more nitrate radical ($NO_3^{\cdot}$, E^0 = 2–2.2 V) showing less reactivity towards SDZ than $^{\cdot}SO_4^-$ could be generated by NO_3^- and $^{\cdot}SO_4^-$ in the presence of nitrate.[39] The effect of chloride on SDZ degradation in the

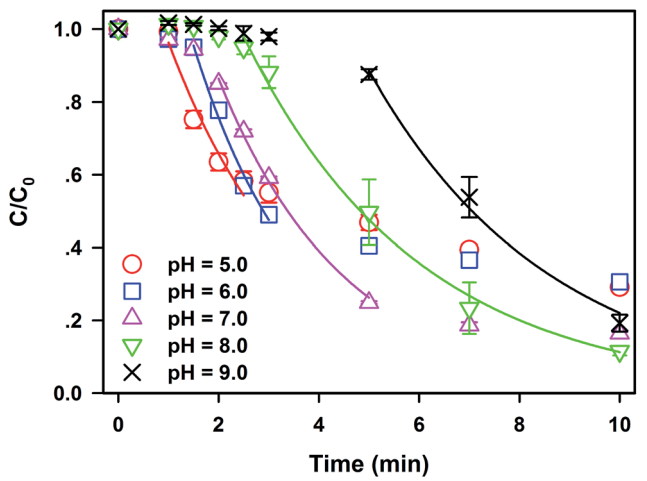

Fig. 2 Effect of initial pH on SDZ degradative kinetics by Fe^0/PS. Experimental conditions: $[Fe^0]_0$ = 1 mM, $[PS]_0$ = 1 mM, [SDZ] = 20 μM, rpm = 600, and T = 20 ± 1 °C.

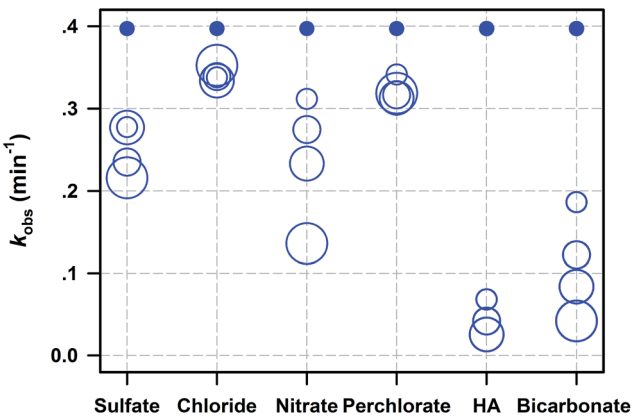

Fig. 3 Summary of k_{obs} for SDZ degradation by Fe0/PS with background materials (dissolved anions and HA). The circle size represents the concentration of each background material. Values of k_{obs} for all these data and different levels of concentrations are given in Table S1.† Reaction conditions: $[Fe^0]_0$ = 1 mM, $[PS]_0$ = 1 mM, [SDZ] = 20 μM, initial pH = 7.0, rpm = 600, and T = 20 ± 1 °C.

Fe^0/PS process was more complicated than other water matrixes. Generally, chlorate exhibited the reaction with $^{\bullet}SO_4^-$ at the rate constant of (1.3–3.1) × 10^8 M^{-1} s^{-1} which could compete for $^{\bullet}SO_4^-$ with SDZ,[8] and SDZ degradative rate was decreased in the presence of chloride. However, chloride could be oxidized to halogenated reactive species such as $Cl^{\bullet}$ and $Cl_2^{\bullet-}$ which still exhibited strong degradative ability to SDZ.[40,41] Thus, the presence of chloride did not seriously inhibit SDZ removal by Fe^0/PS, and a higher concentration of chloride decreased the inhibiting effect of chloride on SDZ degradation. The perchlorate anions inhibited SDZ removal by Fe^0/PS since the perchlorate could occupy some reactivity sites of Fe^0 reacting with PS, which decreased SDZ removal rate.[24] However, the degradative rate of SDZ was not affected as the perchlorate increased to 5 mM. The presence of bicarbonate ranged from 0 to 5 mM significantly inhibited the degradation of SDZ by Fe^0/PS. With increasing HCO_3^-, the final removal rate and k_{obs} both sharply decreased. The negative effect of HCO_3^- on SDZ degradation was most serious among other tested anions. This achieved result was accompany with other reports using activated persulfate process to degrade organic pollutants.[22,30] As Ghauch *et al.*[30] reported, HCO_3^- delayed iron corrosion and limit Fe(II) release into the solution, which could inhibit the generation of ROS in the Fe^0/PS system.

On the other side, HCO_3^- was considered as an active quencher for $^{\bullet}SO_4^-$ and $^{\bullet}OH$ which could compete ROS with SDZ. HA as the most important natural organic matters in surface water and ground water played a critical role on SDZ degradative kinetics by Fe^0/PS. HA was consider as a competitive organic to SDZ in the Fe^0/PS process, and extensively decreased the removal rate of SDZ. Meanwhile, HA also was a strong ligand[13] which could quickly complex dissolving Fe(II) in the Fe^0/PS process and inhibited the reaction between Fe(II) and PS. Overall, all the chosen background materials including Cl^-, SO_4^{2-}, NO_3^-, ClO_4^-, HCO_3^-, and HA inhibited SDZ removal by Fe^0/PS following a trend of $Cl^- < ClO_4^- < SO_4^{2-} < NO_3^- < HCO_3^- <$ HA.

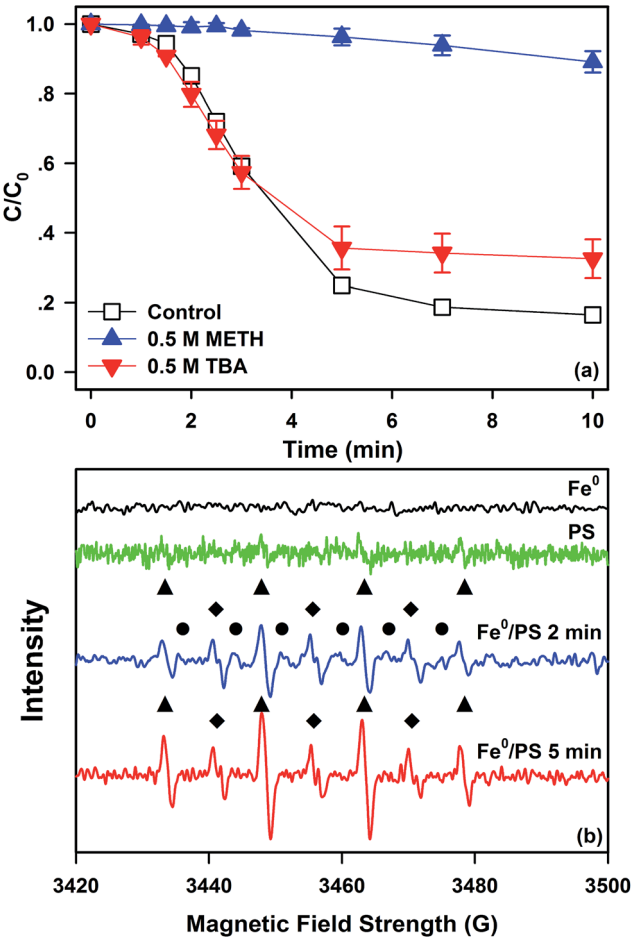

Fig. 4 Inhibition effect of radical quenchers on SDZ degradation in the Fe^0/PS process (a) and ESR spectra obtained from Fe^0, PS, and the Fe^0/PS process with the existence of DMPO (▲ represents the DMPO–$^{\bullet}OH$ adduct, ● represents the DMPO–$^{\bullet}SO_4^-$ adducts, and ◆ represents the HDMPO–OH adduct) (b). Reaction conditions: $[Fe^0]_0$ = 1 mM, $[PS]_0$ = 1 mM, [SDZ] = 20 μM, $[TBA]_0$ or $[METH]_0$ = 500 mM, initial pH = 7.0, rpm = 600, and T = 20 ± 1 °C. EPR experimental conditions: $[DMPO]_0$ ≈ 0.1 M, $[Fe^0]_0$ = 10 mM, $[PS]_0$ = 10 mM, initial pH = 7.0, T = 20 ± 1 °C.

Identification of the ROS in the Fe^0/PS process

Quenching experiments were carried out to identify ROS generated in the Fe^0/PS process. Generally, $^{\bullet}SO_4^-$ is considered as the main ROS in the reactions between PS and Fe(II). Meanwhile, $^{\bullet}OH$ may also be generated by $^{\bullet}SO_4^-$ described in eqn (7) and (8) with the second order rate constant of 10^3–10^4 M^{-1} s^{-1} and 4.6–9.1 M^{-1} s^{-1}, respectively. Besides, the second order constants for methanol (METH) towards $^{\bullet}OH$ and $^{\bullet}SO_4^-$ are 9.7 × 10^8 M^{-1} s^{-1} and 2.5 × 10^7 M^{-1} s^{-1}, and for *tert*-butyl alcohol (TBA) are (3.8–7.6) × 10^8 M^{-1} s^{-1} and (4.0–9.1) × 10^5 M^{-1} s^{-1}, respectively.[42] So METH and TBA were applied to identify the contribution of $^{\bullet}OH$ or $^{\bullet}SO_4^-$ to SDZ degradation by Fe^0/PS.

Degradative kinetics of SDZ by Fe^0/PS in the presence of 500 mM METH and TBA were shown in Fig. 4(a). In the presence of 500 mM METH, the degradation of SDZ was entirely inhibited, and the final removal rate only reached 10.9%. Contrarily, the degradative rate of SDZ by Fe^0/PS decreased to 67.4% with 500 mM TBA. Although TBA exhibited much lower rate constant to $^{\bullet}SO_4^-$, high concentration of TBA could also scavenge partial $^{\bullet}SO_4^-$ in solution. In addition, the difference of inhibiting effects between TBA and METH was considered as the contribution of $^{\bullet}SO_4^-$. Thus, $^{\bullet}SO_4^-$ was considered as the dominated ROS in the Fe^0/PS process.

To further confirm the presence of $^{\bullet}SO_4^-$, EPR spectroscopy was used to verify the specific adduct between DMPO and ROS generated in the Fe^0/PS process. As shown in Fig. 4(b), three apparent signals of DMPO–$^{\bullet}OH$, DMPO–$^{\bullet}SO_4^-$, and HDMPO–OH (the oxidative products of HDMPO by $^{\bullet}OH$) adducts at different time interval in the Fe^0/PS process were detected by EPR. However, no signals of DMPO–$^{\bullet}OH$, DMPO–$^{\bullet}SO_4^-$, HDMPO–OH, and DMPOX (the oxidative products of DMPO by $^{\bullet}OH$) were determined by EPR in Fe^0 or PS solution, which indicated that no ROS could be generated by Fe^0 or PS in experimental conditions. The special hyperfine coupling constants (a(N) 1.49 mT, a(H) 1.49 mT, all ±0.05 mT, 1 : 2 : 2 : 1

quartet) were consistent with that of the DMPO–$^{\cdot}OH$ adduct, while the special hyperfine coupling constants (a(N) 1.38 mT, a(H) 1.02 mT, a(H) 0.14 mT, a(H) 0.08 mT, all ±0.05 mT) were in accordance with that of the DMPO–$^{\cdot}SO_4^-$ adduct.[14] HDMPO was generated by the reaction of Fe(II) and DMPO which was always observed in Fenton reactions.[43] According to literatures,[23,42] the signal of DMPO–$^{\cdot}SO_4^-$ adducts usually accompanied with the signal of DMPO–$^{\cdot}OH$ but hardly to be detected alone in aquatic solution. Besides, the intensity of DMPO–$^{\cdot}SO_4^-$ was much lower than that of DMPO–$^{\cdot}OH$. This behaviour was ascribed to the fast transformation from DMPO–$^{\cdot}SO_4^-$ adducts to DMPO–$^{\cdot}OH$ adducts *via* nucleophilic substitution.[35]

$$^{\cdot}SO_4^- + H_2O \rightarrow {}^{\cdot}OH + SO_4^{2-} + H^+ \quad (7)$$

$$^{\cdot}SO_4^- + OH^- \rightarrow {}^{\cdot}OH + SO_4^{2-} \quad (8)$$

Discussion on the role of Fe^0 in the Fe^0/PS process

As mentioned above, $^{\cdot}SO_4^-$ might be produced *via* two different reactions of eqn (1) and eqn (5). Hereon, the key role of Fe^0 in the Fe^0/PS process should be clarified to understand mechanisms of SDZ removal by Fe^0/PS. As shown in Fig. 5(a), 1,10-phenanthroline as an excellent complex with Fe(II) has been added to study SDZ degradative kinetics by Fe^0/PS.[44] A very critical inhibition of SDZ removal was observed in the presence of 1 mM 1,10-phenanthroline, and as 1,10-phenanthroline increased to 5 mM, the degradation of SDZ almost was completely stopped by blocking the reaction of eqn (1) since the complex of Fe(II) with 1,10-phenanthroline extensively decreased the concentration of dissolved Fe(II). Meanwhile, the presence of 1,10-phenanthroline did not inhibit the reaction between Fe^0 and PS (Eq. (5)) which indicated that $^{\cdot}SO_4^-$ might not be produced *via* the direct oxidation of Fe^0 by PS. Although EDTA was a good ligand for Fe(II) and Fe(III), EDTA was considered as a common promoter in reactions based on $^{\cdot}OH$ especially in Fe^0/O_2 reactions.[27,45] As illustrated in Fig. 5(b), various level of EDTA concentrations ranged from 0.05 to 5 mM all inhibited SDZ degradation by Fe^0/PS. EDTA was the complex of Fe(II) which exhibited the similar effects on SDZ degradation to 1,10-phenanthroline. EDTA was an organics which could compete $^{\cdot}SO_4^-$ with SDZ. Therefore, the negative effect of EDTA in the Fe^0/PS process is different from that in Fe^0/O_2 reactions.

Dissolving oxygen (DO) in solution also played a significant role in the Fe^0/PS system[29] by changing the corrosion of Fe^0. Kinetics experiments of SDZ removal by Fe^0/PS conducted in the presence of N_2, air, and O_2 are shown in Fig. 5(c). Anoxic conditions could enhanced SDZ removal by Fe^0/PS; nevertheless, the presence of excess oxygen could depress the SDZ degradation. According to the mechanisms of Fe^0/PS *via* the indirect reaction between Fe(II)/PS, the release of Fe(II) was the rate-limiting step. By comparing to the experiments with air or oxygen, dissolving Fe(II) was more stable without the generation of iron oxides on Fe^0 surface in the presence of N_2, which could promote generation of ROS *via* eqn (1). Meanwhile, the lower SDZ removal rate in the presence of air and oxygen indicated

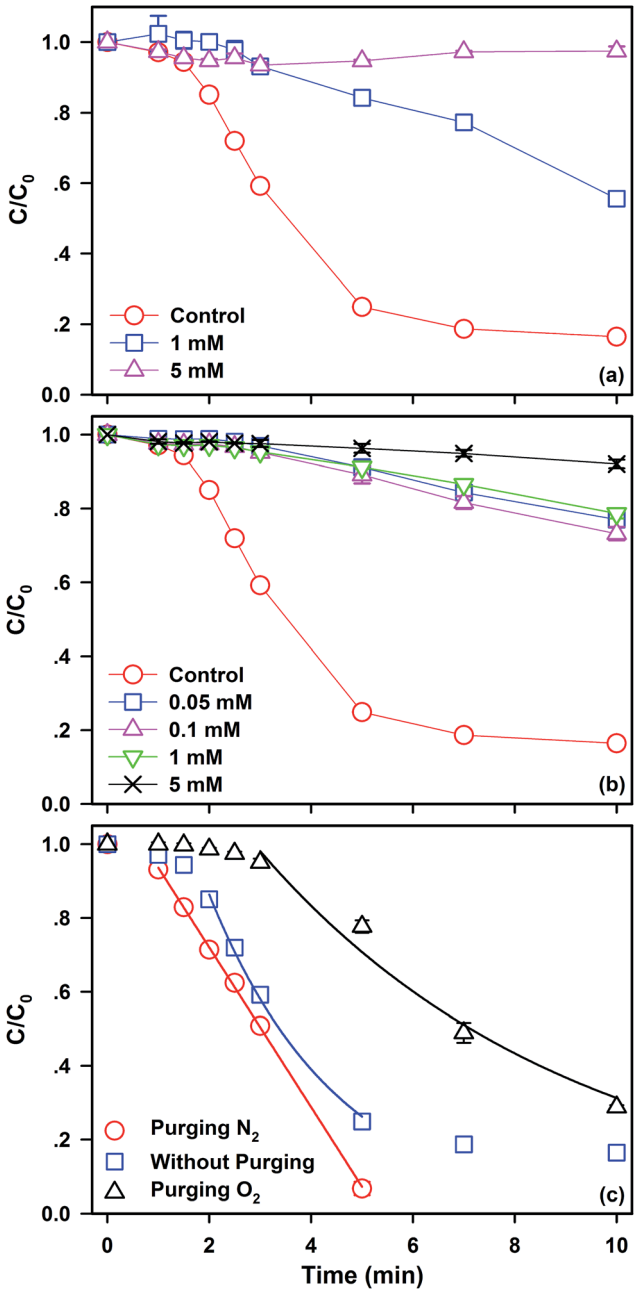

Fig. 5 Effects of 1,10-phenanthroline (a), EDTA (b), and DO (c) on SDZ degradation in the Fe^0/PS process. Reaction conditions: $[Fe^0]_0 = 1$ mM, $[PS]_0 = 1$ mM, [SDZ] = 20 μM, initial pH = 7.0, rpm = 600, and $T = 20 \pm 1$ °C.

that the generation of $^{\cdot}OH$ by Fe^0 and O_2 might be ignored in the Fe^0/PS process. Besides, the lag phase with purging oxygen increased to 3 min. Although the inhibition of DO on SDZ removal might be assumed to the lack of Fe^0 which decreased the generation of ROS *via* eqn (5), the consumption of Fe^0 could not extend the lag phase of reactions. Thus, the extending lag phase increasing with the concentration of DO was ascribed to the generation of iron oxides by the oxidation of Fe(II) by oxygen on the iron surface, which blocked the reactions between Fe(II) and PS.

Table 1 Charges (q_i) and f_i^0 of atoms in SDZ molecule ($N+1$ and $N-1$)

Atom, i	q_{N-1}	q_{N+1}	f_i^0
C1	0.069	−0.007	0.038
C2	−0.087	0.036	−0.062
C3	0.170	0.201	−0.016
N4	−0.278	−0.212	−0.033
C5	0.342	0.390	−0.024
N6	−0.272	−0.320	0.024
N7	−0.210	−0.251	0.020
S8	1.304	0.527	0.388
O9	−0.752	−0.867	0.058
O10	−0.740	−0.851	0.055
C11	0.350	0.007	0.171
C12	−0.010	0.031	−0.021
C13	−0.040	−0.389	0.174
C14	0.169	0.400	−0.115
C15	−0.030	−0.047	0.008
C16	0.034	0.004	0.015
N17	−0.076	−0.297	0.111

Possible degradation pathways of SDZ by Fe^0/PS

Many studies have identified the degradation intermediates of SDZ by various processes including ozonation,[5] Fenton,[46] and US/Fe^0/PS systems.[2] The species of reaction intermediates and degradation pathways of SDZ in different AOPs identified by GC-MS, LC-MS, and HPLC were different. In this paper, off line SPE-UHPLC-MS was utilized to detect the reaction intermediates of SDZ by Fe^0/PS at pH 7.0, based on which the SDZ degradation pathways were proposed.

As literatures reported, N7, N11, N13 and N17 in SDZ might be reactive sites for oxidation. To confirm the theoretical reactive sites in SDZ molecule, Fukui function calculations of f_i^0 was employed to assign the most vulnerable sites of SDZ by the attack of $^{\cdot}SO_4^-$ radical. f_i^0 was calculated by eqn (9)[47] which obtained by Multiwfn software based on Hirshfeld charges.[48] Thus, Hirshfeld charges and calculated values of condensed Fukui function (f_i^0) of the optimized SDZ molecule ($N+1$ and $N-1$) are listed in Table 1. According to the value of condensed Fukui function (f_i^0), atoms of S8, O8, O9, C13, C11, N17, C1, N6, and N7 were the most reactive sites for $^{\cdot}SO_4^-$ radical attack.

$$f_i^0 = \frac{\left(q_i^{N-1} - q_i^{N+1}\right)}{2} \quad (9)$$

where i, q, f, and N represent the atom in SDZ molecule, the charge of the atom (i), the value of condensed Fukui function, and the number of electrons of SDZ, respectively.

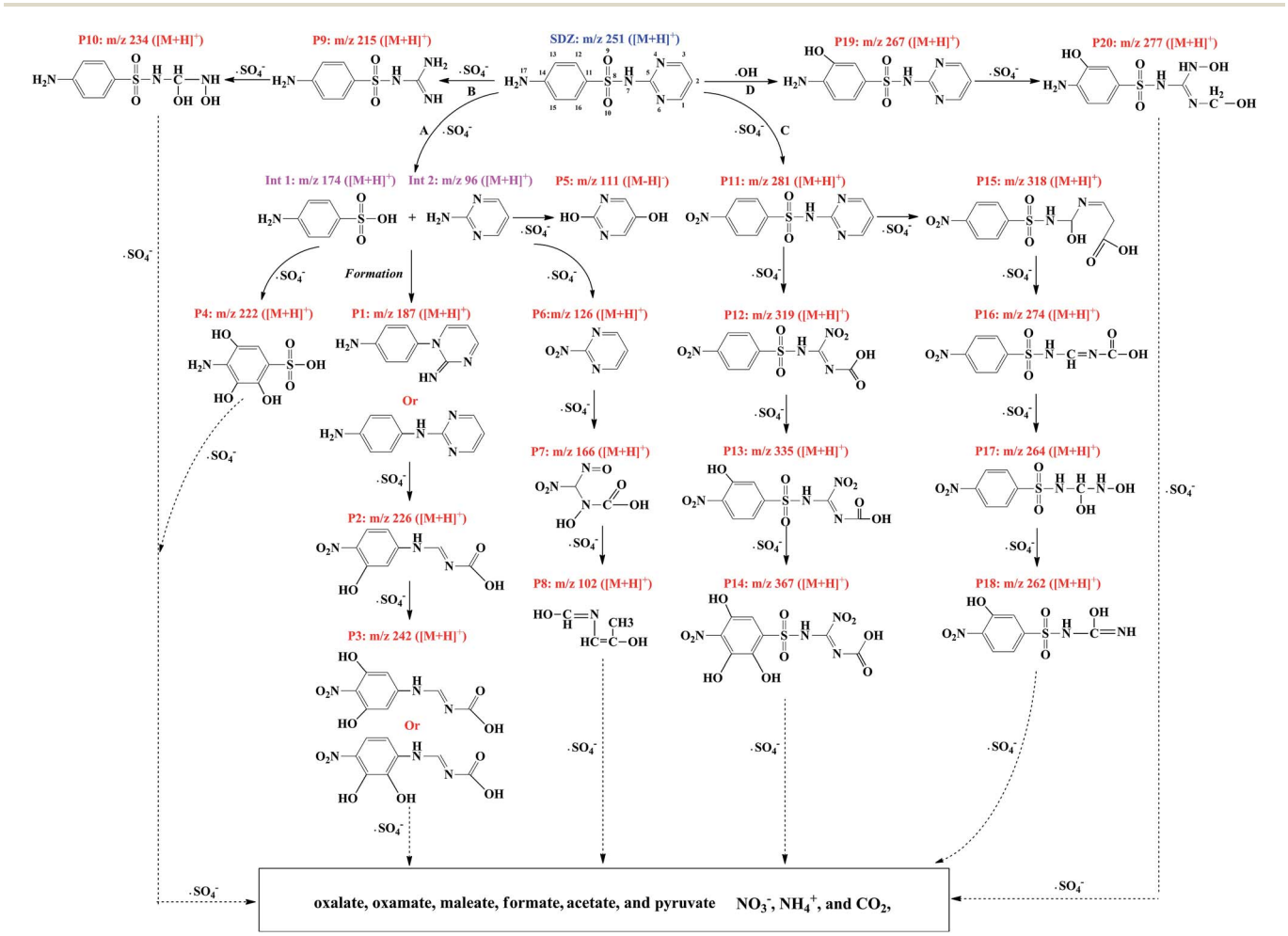

Fig. 6 Possible degradation pathways of SDZ by Fe^0/PS.

By combination of full scan and product ion mode, 20 reaction intermediates and SDZ were detected in the process of SDZ removal by Fe^0/PS, which were all illustrated from Fig. S6 to Fig. S26.† Based on the detected intermediates specified in this study, four proposed transformation pathways (A, B, C, and D) of SDZ degradation in the Fe^0/PS process were presented in Fig. 6. Pathway A was formed *via* the break of S8–N7 bond by $^{\cdot}SO_4^-$ radical, and 4-aminobenzenesulfonic acid (Int 1) and pyrimidin-2-amine (Int 2) were generated. By the continuous attacking of $^{\cdot}SO_4^-$ to Int 1, 4-amino-2,3,5-trihydroxybenzenesulfonic acid (P4, m/z^+ 222) was produced. Meanwhile, 2-nitropyrimidine (P6, m/z^+ 126) was formed by the oxidation of Int 2 by $^{\cdot}SO_4^-$, and hydroxy(nitro(nitroso)methyl) carbamic acid (P7, m/z^+ 166) and *N*-((*E*)-2-hydroxyprop-1-en-1-yl) formimidic acid (P8, m/z^+ 102) also were detected as the oxidative products of P6. Besides, the formation of 4-(2-iminopyrimidin-1(2*H*)-yl) aniline or *N*-(pyrimidin-2-yl) benzene-1,4-diamine (P1, m/z^+ 187) between Int 1 and Int 2 was also a common reaction in SDZ degradation by $^{\cdot}SO_4^-$.[49] In addition, the oxidative pathway of P1 by $^{\cdot}SO_4^-$ was also established based on the detection of P2 (m/z^+ 226) and P3 (m/z^+ 242).

In pathway B and C, direct attacking of $^{\cdot}SO_4^-$ on N6 and N17 produced 4-amino-*N*-carbamimidoyl benzenesulfonamide (P9, m/z^+ 215) and 4-nitro-*N*-(pyrimidin-2-yl)benzenesulfonamide (P11, m/z^+ 281),[2] respectively. And P9 was oxidized to 4-amino-*N*-(hydroxy(hydroxyamino)methyl)benzenesulfonamide (P10, m/z^+ 234) by $^{\cdot}SO_4^-$. P11 was the most frequently oxidative product of SDZ by $^{\cdot}SO_4^-$.[2] Besides, abundant oxidative products of P11 by $^{\cdot}SO_4^-$ are also detected and illustrated in Fig. 6.

Among three pathways of SDZ degradation *via* $^{\cdot}SO_4^-$, the products generated by pathway A was more abundant than pathway B and C. As shown in Fig. S27,† four initial products of P1, P4, P5, and P6 in pathway A were detected in the first 2 min. All four products increased with reaction time, and then decreased, which revealed that pathway A could continuously consume $^{\cdot}SO_4^-$. Besides, the area of P11 in pathway B increased with reaction time, which proved that pathway B, was also important to the removal of SDZ. However, P9 of pathway C was firstly detected at 5 min, which indicated the contribution of attacking on N6 by $^{\cdot}SO_4^-$ was ignored in the first 5 min.

Pathway D was a classical oxidative pathway of SDZ by $^{\cdot}OH$ but was hardly to be formed in oxidative systems based on $^{\cdot}SO_4^-$. The generation of OH-SDZ (P19, m/z^+ 267)[2] by substituting H at C13 with hydroxyl indicated that $^{\cdot}OH$ also joined the degradation of SDZ in the Fe^0/PS process. In addition, the contribution of pathway D to SDZ removal was consistent with the experiments of identifying ROS, which was about 16.1%.

Conclusions

Batch experiments were carried out to investigate effects of some key factors on SDZ removal by Fe^0/PS. Initial concentrations of Fe^0 and PS increased from 0.25 to 5 mM both increased the removal rate of SDZ. But increasing SDZ inhibited the SDZ removal rate for the limitation of ROS. Neutral or weak alkaline solutions exhibited higher removal rate of SDZ than weak acid pH, which indicated that the Fe^0/PS process was a potential technology for engineering applications in organics removal. Common aquatic matrixes including sulfate, nitrate, chloride, perchlorate, bicarbonate, and HA all showed negative effects on SDZ degradation in the Fe^0/PS process following a trend of $Cl^- < ClO_4^- < SO_4^{2-} < NO_3^- < HCO_3^- <$ HA. To verify the dominating ROS in the Fe^0/PS system, chemical quenching experiments in the presence of METH and TBA were conducted. Results of quenching experiments implied that $^{\cdot}SO_4^-$ was the dominating ROS in the Fe^0/PS system. The chemical detection of DMPO–$^{\cdot}SO_4^-$ and DMPO–$^{\cdot}OH$ by EPR spectra also confirmed the presence of $^{\cdot}SO_4^-$. Besides, strongly negative effects of 1,10-phenanthroline and EDTA on SDZ degradation in the Fe^0/PS process proved that $^{\cdot}SO_4^-$ was not generated by an one-step reaction between Fe^0 and PS but *via* the indirect oxidation of Fe(II) by PS. Meanwhile, the negative effect of DO on SDZ removal also proved that the generation of $^{\cdot}SO_4^-$ was dominated by reactions between Fe(II) and PS. Finally, three pathways *via* $^{\cdot}SO_4^-$ attack and one pathway *via* $^{\cdot}OH$ substitute of SDZ degradation by Fe^0/PS were proposed based on the reactive sites attacking by radicals and intermediate products.

Conflicts of interest

There are no conflicts to declare.

Acknowledgements

We gratefully acknowledge Mr Juanshan Du (State Key Laboratory of Urban Water Resource and Environment, Harbin Institute of Technology, Harbin, PR China) for the kind supporting of chemical calculations and EPR experiments.

References

1 Q. Q. Zhang, G. G. Ying, C. G. Pan, Y. S. Liu and J. L. Zhao, *Environ. Sci. Technol.*, 2015, **49**, 6772–6782.
2 X. Zou, T. Zhou, J. Mao and X. Wu, *Chem. Eng. J.*, 2014, **257**, 36–44.
3 L. Y. He, Y. S. Liu, H. C. Su, J. L. Zhao, S. S. Liu, J. Chen, W. R. Liu and G. G. Ying, *Environ. Sci. Technol.*, 2014, **48**, 13120–13129.
4 W. Q. Guo, R. L. Yin, X. J. Zhou, J. S. Du, H. O. Cao, S. S. Yang and N. Q. Ren, *Ultrason. Sonochem.*, 2015, **22**, 182–187.
5 W. Guo, Z. Yang, J. Du, R. Yin, X. Zhou, S. Jin and N. Ren, *RSC Adv.*, 2016, **6**, 57138–57143.
6 W. Baran, E. Adamek, A. Sobczak and A. Makowski, *Appl. Catal., B*, 2009, **90**, 516–525.
7 Y. Luo, D. Mao, M. Rysz, Q. Zhou, H. Zhang, L. Xu and P. J. J. Alvarez, *Environ. Sci. Technol.*, 2010, **44**, 7220–7225.
8 T. Zhou, X. Zou, J. Mao and X. Wu, *Appl. Catal., B*, 2016, **185**, 31–41.
9 O. Gonzalez, C. Sans and S. Esplugas, *J. Hazard. Mater.*, 2007, **146**, 459–464.
10 M. Clara, B. Strenn, O. Gans, E. Martinez, N. Kreuzinger and H. Kroiss, *Water Res.*, 2005, **39**, 4797–4807.

11 X. M. Xiong, Y. K. Sun, B. Sun, W. H. Song, J. Y. Sun, N. Y. Gao, J. L. Qiao and X. H. Guan, *RSC Adv.*, 2015, **5**, 13357–13365.
12 X. Guo, Z. Yang, H. Dong, X. Guan, Q. Ren, X. Lv and X. Jin, *Water Res.*, 2016, **88**, 671–680.
13 J. S. Du, B. Sun, J. Zhang and X. H. Guan, *Environ. Sci. Technol.*, 2012, **46**, 8860–8867.
14 J. Zou, J. Ma, L. Chen, X. Li, Y. Guan, P. Xie and C. Pan, *Environ. Sci. Technol.*, 2013, **47**, 11685–11691.
15 A. Ghauch, *J. Adv. Oxid. Technol.*, 2017, **20**, 20160197–20160198.
16 S. Naim and A. Ghauch, *Chem. Eng. J.*, 2016, **288**, 276–288.
17 A. Ghauch, A. M. Tuqan, N. Kibbi and S. Geryes, *Chem. Eng. J.*, 2012, **213**, 259–271.
18 Y. Wang, J. B. Liang, X. D. Liao, L.-s. Wang, T. C. Loh, J. Dai and Y. W. Ho, *Ind. Eng. Chem. Res.*, 2010, **49**, 3527–3532.
19 X. Xiong, B. Sun, J. Zhang, N. Gao, J. Shen, J. Li and X. Guan, *Water Res.*, 2014, **62**, 53–62.
20 A. Ghauch, A. M. Tuqan and N. Kibbi, *Chem. Eng. J.*, 2015, **279**, 861–873.
21 A. Ghauch, A. Baalbaki, M. Amasha, R. El Asmar and O. Tantawi, *Chem. Eng. J.*, 2017, **317**, 1012–1025.
22 P. Neta, R. E. Huie and A. B. Ross, *J. Phys. Chem. Ref. Data*, 1988, **17**, 1027–1284.
23 C. Qi, X. Liu, Y. Li, C. Lin, J. Ma, X. Li and H. Zhang, *J. Hazard. Mater.*, 2017, **328**, 98–107.
24 J. Du, D. Che, X. Li, W. Guo and N. Ren, *RSC Adv.*, 2017, **7**, 18231–18237.
25 L. P. Liang, X. H. Guan, Z. Shi, J. L. Li, Y. N. Wu and P. G. Tratnyek, *Environ. Sci. Technol.*, 2014, **48**, 6326–6334.
26 L. P. Liang, W. Sun, X. H. Guan, Y. Y. Huang, W. Y. Choi, H. L. Bao, L. N. Li and Z. Jiang, *Water Res.*, 2014, **49**, 371–380.
27 X. H. Guan, Y. K. Sun, H. J. Qin, J. X. Li, I. M. Lo, D. He and H. R. Dong, *Water Res.*, 2015, **75**, 224–248.
28 L. J. Matheson and P. G. Tratnyek, *Environ. Sci. Technol.*, 1994, **28**, 2045–2053.
29 G. Ayoub and A. Ghauch, *Chem. Eng. J.*, 2014, **256**, 280–292.
30 A. Ghauch, G. Ayoub and S. Naim, *Chem. Eng. J.*, 2013, **228**, 1168–1181.
31 S. Y. Oh, S. G. Kang and P. C. Chiu, *Sci. Total Environ.*, 2010, **408**, 3464–3468.
32 X. Guo, Z. Yang, H. Liu, X. Lv, Q. Tu, Q. Ren, X. Xia and C. Jing, *Sep. Purif. Technol.*, 2015, **146**, 227–234.
33 Z. Xiong, B. Lai, P. Yang, Y. Zhou, J. Wang and S. Fang, *J. Hazard. Mater.*, 2015, **297**, 261–268.
34 Y. Yuan, B. Lai and Y. Y. Tang, *Chem. Eng. J.*, 2016, **283**, 1514–1521.
35 T. Zhou, Y. Li, J. Ji, F. S. Wong and X. Lu, *Sep. Purif. Technol.*, 2008, **62**, 551–558.
36 T. Sugimoto and Y. S. Wang, *J. Colloid Interface Sci.*, 1998, **207**, 137–149.
37 X. Wu, X. Gu, S. Lu, Z. Qiu, Q. Sui, X. Zang, Z. Miao and M. Xu, *Sep. Purif. Technol.*, 2015, **147**, 186–193.
38 W. Z. Yin, J. H. Wu, P. Li, X. D. Wang, N. W. Zhu, P. X. Wu and B. Yang, *Chem. Eng. J.*, 2012, **184**, 198–204.
39 P. Neta and R. E. Huie, *J. Phys. Chem.*, 1986, **90**, 4644–4648.
40 R. Yuan, S. N. Ramjaun, Z. Wang and J. Liu, *J. Hazard. Mater.*, 2011, **196**, 173–179.
41 C. Liang, Z. S. Wang and N. Mohanty, *Sci. Total Environ.*, 2006, **370**, 271–277.
42 G. Fang, J. Gao, D. D. Dionysiou, C. Liu and D. Zhou, *Environ. Sci. Technol.*, 2013, **47**, 4605–4611.
43 J. M. Fontmorin, R. C. Burgos Castillo, W. Z. Tang and M. Sillanpaa, *Water Res.*, 2016, **99**, 24–32.
44 L. P. Liang, W. J. Yang, X. H. Guan, J. L. Li, Z. J. Xu, J. Wu, Y. Y. Huang and X. Z. Zhang, *Water Res.*, 2013, **47**, 5846–5855.
45 C. R. Keenan and D. L. Sedlak, *Environ. Sci. Technol.*, 2008, **42**, 6936–6941.
46 J. F. Yang, S. B. Zhou, A. G. Xiao, W. J. Li and G. G. Ying, *J. Environ. Sci. Health, Part B*, 2014, **49**, 909–916.
47 J. Oláh, C. Van Alsenoy and A. B. Sannigrahi, *J. Phys. Chem. A*, 2002, **106**, 3885–3890.
48 F. L. Hirshfeld, *Theor. Chim. Acta*, 1977, **44**, 129–138.
49 Y. Feng, D. Wu, Y. Deng, T. Zhang and K. Shih, *Environ. Sci. Technol.*, 2016, **50**, 3119–3127.